

## A Micro-Biomanipulation Training System based on Mixed-Reality

Leonardo S. Mattos, Darwin G. Caldwell

Advanced Robotics Department  
Italian Institute of Technology (IIT)  
Genoa, Italy

{leonardo.demattos, darwin.caldwell}@iit.it

**Abstract**— Within neuroscience, micromanipulation and microinjection of cells (blastocysts and neurons) are essential and highly skilled tasks that can require years of training. These tasks are traditionally performed via direct manual control of the biomanipulation equipment while looking through a microscope. Yet, even after extensive training, yield can be low (40 – 70%). This paper presents a mixed-reality system for the training of operators (biologists/neuroscientists) on a new fully teleoperated biomanipulation system with reduced training requirements and much higher yields. Two mixed-reality training scenarios were designed, implemented and tested for this purpose: A “move-and-inject” task focused on precise positioning training; and a trajectory following scenario intended to develop precise motion control skills in new operators. Preliminary experiments performed with 20 totally novice operators demonstrate that this new training system is effective in terms of the initial development of control skills for real teleoperated biomanipulations. Experimental metrics demonstrate an exponential learning curve for these novice operators, who achieve good performance values after only two practice runs on the system. In addition, this training is shown to be safe and inexpensive since no real cells, biochemical products, or several pipettes are needed for this initial training phase.

**Keywords**-mixed-reality; teleoperation; biomanipulation; micromanipulation

### I. INTRODUCTION

Biomanipulation, in the context of this work, involves the transportation, orientation and injection of microscopic biological structures such as single cells and early embryos. These operations are normally performed under high-magnification microscopes using glass pipettes with very fine tips (2-50 $\mu$ m), which are attached to micromanipulators and microinjectors. Micromanipulators are mechanical or electro-mechanical devices that scale down the operator’s motions to enable precise control of tools in the micrometer range. Microinjectors are devices used for precise control of fluid motion inside the pipettes.

Modern biomanipulation devices are motorized and capable of high-resolution control. For example, commonly used Eppendorf equipment, such as the TransferMan NK2 micromanipulator and the FemtoJet microinjector, offer motion resolution down to 40nm and the capability of injecting volumes down to the femtolitre into cells. However, under direct operator control these high-resolution

motion capabilities are difficult to achieve and do not easily translate into accurate control and successful manipulations.

As a result of these operational difficulties the training period required to achieve proficiency in biomanipulations is normally high, reaching up to one year for operations such as embryo microinjection [2]. In addition, the training process is expensive, involving not only the costs of the underperforming operator, but also expenses associated with wasted materials, samples preparation, cell culture, etc. Furthermore, even after extensive training, the success rates of biomanipulations are found to be less than ideal (40 - 70% for embryo microinjections [3]), pointing to problems related to the user interface and ergonomic factors of the microscope/micromanipulation setup [4]. Typical issues include: high susceptibility to human errors, such as unintentional erroneous motions; and the tiring working conditions, where operators spend hours looking through microscopes while simultaneously controlling micromanipulators and microinjectors.

Improvements to the biomanipulation setup and to its control interface can be achieved using teleoperation techniques whereby the operator controls the system from a computer station, looking at the live video captured from the microscope and displayed on the computer screen. The control of the micromanipulators can be accomplished through the computer keyboard [5]; game joysticks [6]; or even through haptic devices [7][8].

A teleoperated system has the potential to greatly improve biomanipulations by offering supervised control of the micromanipulator motions, which can filter hand tremors and even block erroneous motions [9][10]. In addition, a single teleoperated system can offer different control modalities for the micromanipulators, including position [11], velocity [6] and force control [12], which can be selected according to the specific biomanipulation task or user preference. Furthermore, the speed and precision of the micromanipulator can be dynamically adjusted in a teleoperated system, both automatically [13][14] or manually, further improving manual operations.

Additional benefits of a teleoperated biomanipulation system include the automatic execution of motions that are virtually impossible under direct manual control of the micromanipulators. Examples are simultaneous motions in three dimensions, e.g. fast and precise motions such as “stabbing” movements used to penetrate some cells; and slow linear motions often desired for retracting the pipette from injected cells along the entry path. Another obvious

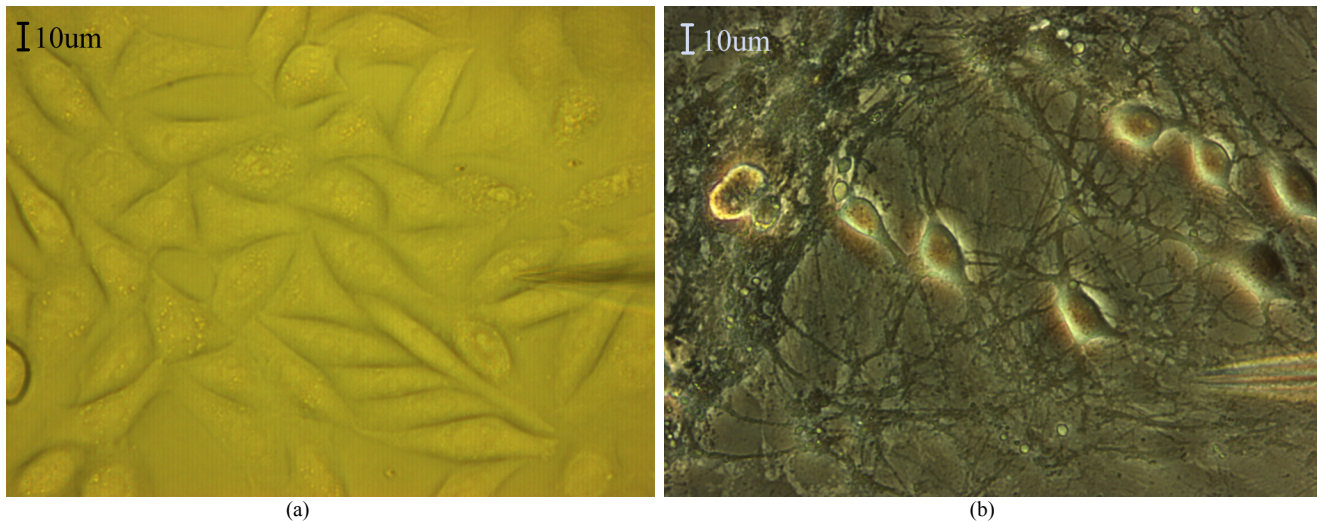


Fig.1. (a) Microinjection of CHO-K1 cells under bright-field imaging. (b) Microinjection of neurons using phase contrast imaging. Scale bars on the pictures read 10µm. The diminutive size of these adherent cells require the use of high-magnification objectives, complicating precise pipette positioning over the target cells due to the shallow focal depth of these lenses.

benefit is the creation of a more ergonomic and intuitive work environment by careful arrangement of the display screen and the interfaces to enhance hand-eye collocation and co-ordination. This is less tiring, since the operator can sit comfortably in front of a computer display. In fact, this is a familiar environment to most people, including new operators that should learn biomanipulation tasks, making us hypothesize that teleoperation can enable faster learning at least in part due to this simple reason.

Mixed-reality systems have been developed and used in teleoperations to achieve a diverse range of goals. For instance, they have been used to increase the safety of operations through the creation of virtual barriers in the operating field [10][15]; and also to assist in cell microinjection tasks by providing a preferred direction of motion [3]. Mixed reality has also been used in predictive displays, assisting the planning and execution of robot motions [16]; and in nanomanipulations to provide “haptic” sense in intangible tasks [17]. They have also been used in many training systems for tasks varying from aircraft piloting [18] to minimally invasive surgery [19].

The use of an assistive mixed-reality system can also improve the training and the yield of biomanipulations. For example, our teleoperated system [6] allows the definition of operating zones directly on the live video display, which are used to dynamically adjust the speed and precision of the micromanipulator during operation. This is useful to prevent errors and contributes to increased operation yields because the micromanipulator precision can be automatically increased when the biomanipulation pipette is near a target cell or a danger area.

This paper focuses on the training benefits of a mixed-reality biomanipulation system. Our goal is to show that initial operator training can be done “off-line,” without the need for real cells, biochemical products, or the numerous pipettes that are needed when learning biomanipulations on the traditional manually controlled systems. To this end, a

fully teleoperated biomanipulation system [6] was used as the real setting for operator training, and target cells were replaced by virtual targets and virtual obstacles. Training was performed in two different mixed-reality scenarios: A move-and-inject task focused on training precise pipette positioning; and a trajectory following scenario, intended to train operators on precise control of the pipette motions. Evaluation of training metrics from 20 totally novice operators are presented here, showing that user learning improved exponentially and demonstrating the great value of this mixed-reality training system.

## II. BIOMANIPULATION TASKS

Within the broad field of biomanipulation and particularly microinjection, which is the primary focus of this research, two tasks are of special interest due to their importance and frequency in neuroscience research: adherent cell microinjections and blastocyst microinjections.

Adherent cell microinjection is a delicate and complicated operation that involves the manipulation of cells with dimensions down to 10µm. Figure 1(a) shows adherent cells commonly used in biological and medical

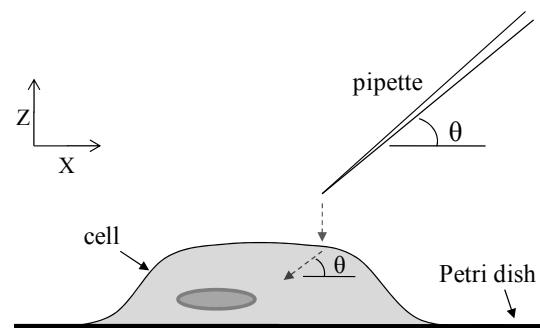


Fig. 2. Synchronized motions on the X- and Z-axis are necessary to create a linear microinjection action when the pipette is positioned on an angle.

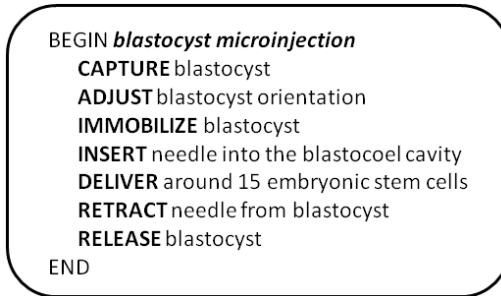
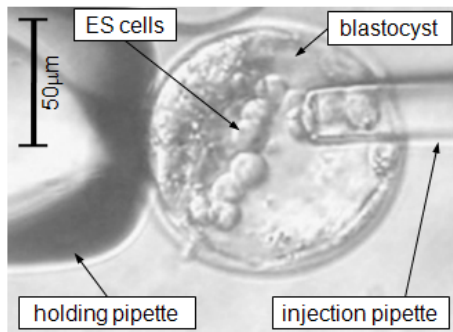


Fig. 3. Blastocyst microinjection and high-level algorithm describing this delicate operation. Coordinated and meticulous control of two micromanipulators and two microinjectors is required in this case, making this operation difficult to master and characterizing its results by low success rates.

research, the CHO-K1 cells [20]. Other examples are neurons, as in Fig.1(b), and endothelial cells. Since these cells adhere to the bottom of the Petri dish, only one pipette/micromanipulator is required to perform the microinjections. However, the pipette needs to be lifted when moving from one cell to another to avoid collisions with other cells and pipette tip breakage. Then, the pipette should be precisely positioned on the upper surface of the next target cell. This operation is complicated by the fact that the diminutive cells require the use of microscope objectives with high magnification factors (40 - 100x), which have a shallow focal depth. This means the pipette tip goes completely out of focus when lifted, making precise positioning difficult. In addition, the injection motion involves simultaneous and coordinated motion in two axes when 3-axis micromanipulators are used, e.g., injection at angle from the top involves simultaneous motions in X and Z (see Fig. 2).

Blastocyst microinjections can be considered as a form of suspension cell microinjection, even though the blastocysts (early embryos) are composed of many cells. In this case, the (mouse) blastocyst moves freely on the bottom of the Petri dish, so injection normally requires the use of two moveable pipettes: one to hold the blastocyst; and the second to perform the actual injection. Figure 3 shows this operation, from which it can be seen that mice blastocysts, measuring around 100µm in diameter, are much larger than the adherent cells mentioned above. Nonetheless, blastocyst microinjections are equally delicate and difficult since even a small error can kill the embryo. One complication here comes from the fact that this task requires coordinated control of two micromanipulators; and another from the need to also control two microinjectors. These complications contribute to increasing the training time required to attain proficiency on this operation, which can typically take up to one year.

As a result of the long training periods and susceptibility to small errors, our research aims at increasing the consistency and efficiency rates attained in manually controlled operations through assisted teleoperation. Consequently, we have developed a teleoperated system that allows easy and precise control of the entire biomanipulation setup from a user-friendly interface.

Nonetheless, efficient operation of this new system also requires some training to attain optimum performance, which motivated the development of the mixed-reality training system described in this paper. The next sections present the system created, the training procedure, and initial training experiments performed with completely novice operators.

### III. BIOMANIPULATION SYSTEM CONFIGURATION

The teleoperated biomanipulation system used in this research was created by the integration of high-end commercial equipment commonly found in neuroscience research laboratories. This was done in favor of: 1) creating a flexible system applicable to a large range of biomanipulation applications; 2) minimizing extra investment from the laboratories that already possess biomanipulation equipment; and 3) increasing the system's acceptance by the biology/neuroscience community, which is already familiar with and trusts the equipment used.

Equipment selection and configuration was performed in collaboration with neuroscience researchers. Based on the mix of their research needs with engineering specifications for automation, the developed system included:

- one Leica DMI6000B inverted microscope
- two Eppendorf TransferMan NK2 motorized micromanipulators
- one Eppendorf Femtojet microinjector
- one Marzhauser SCAN IM 120x100 motorized scanning microscope stage
- two Eppendorf CellTram Vario microinjectors incorporating custom computer-controlled driving systems
- a desktop computer with an Intel Core2 Quad 2.83 GHz CPU, WindowsXP, and 3GB RAM
- an AVT Guppy F-080C firewire camera
- two Saitek Cyborg Evo Force joysticks

These devices are shown in Fig. 4, which presents the two workstations that constitute the developed teleoperated biomanipulation system: The microscope station and the control station.

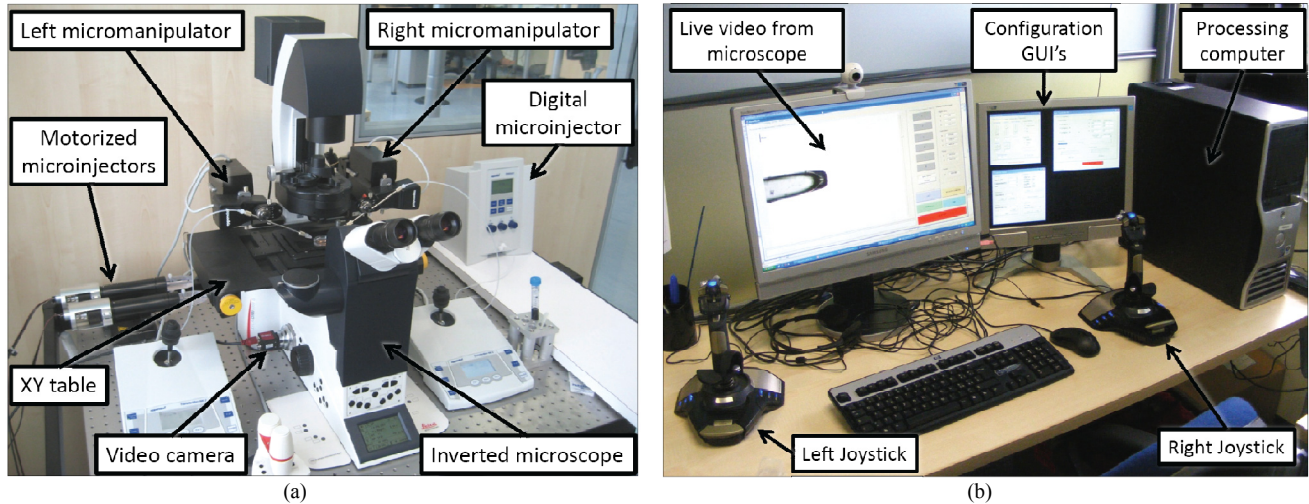


Fig. 4. Teleoperated biomanipulation system configuration: (a) the microscope station; (b) the computer/control station.

The selected devices are appropriate for many different biomanipulation procedures, including the microinjection of blastocysts and adherent cells. These operations can be precisely performed using the selected micromanipulators (which have three translation axes with resolution of 40nm and a maximum speed of 7.5 mm/s) and the FemtoJet microinjector, which can deliver volumes down to the femtolitre.

#### IV. SYSTEM CONTROL AND TELEOPERATION

Control and teleoperation of the devices were achieved through standard 2-way communication interfaces, including RS-232C and CAN. This was possible because all of the selected devices supported external control through a serial communications port. Therefore, the type of connection between the controlling computer and a system device was dictated by the device's supported interface.

All system devices were integrated by software, and could be simultaneously controlled from a graphical user

interface (GUI) running on the desktop computer (see Fig. 5). User commands were received via the joysticks, computer mouse or computer keyboard. These commands were processed and then forwarded to the appropriate biomanipulation equipment.

Feedback from the micro-world was obtained through the video camera, which provided live video feed from the microscope's field of view.

The virtual features used during this research were created using graphics overlaid on the live video stream. The interaction of these virtual features with real system components created the mixed-reality biomanipulation environment. These interactions were enabled by mapping the micromanipulator coordinates to the image space, as described in [21] and summarized below. Using this mapping the system was able to compute the image coordinates of the tool (pipette) without the need for image-based localization software. This created a robust and fast system capable of generating an operating environment influenced by both real and virtual objects. Figure 5 shows some of the virtual features that could be created, including;

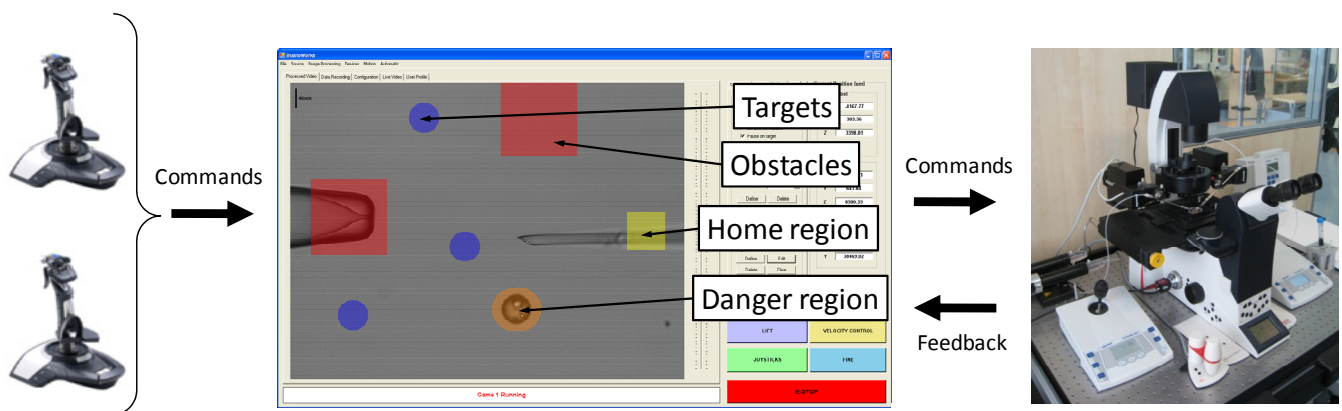


Fig. 5. The mixed-reality biomanipulation system setup and examples of virtual features defined on the operating environment.

targets, obstacles and a danger region. All regions were customizable in terms of maximum speed allowed and repelling force. These virtual components were the basis of the two mixed-reality training scenarios described in section V.

#### A. System Calibration

The calibration procedure used to compute the mapping between the video and robot coordinate frames assumed zero image distortion by the system optics and perfect parallelism between the camera plane and the robot's X-Y plane. Considering these two simplifying assumptions, the calibration procedure consisted of finding the translation, rotation and scaling factors required to map points between the two frames. This was realized by requesting the user to click on the tool tip seen on the live video at five different robot locations. These operations defined  $\{P_0, P_1, P_2, P_3, P_4\}$ , five reference points described with coordinates  ${}^V P_n$  in the video frame and  ${}^R P_n$  in the robot frame. The first two points were initially used to compute the rotation,  $\theta$ , between the coordinate frames according to the method described in Fig. 6; and later to compute the frame transformation described by:

$${}^V P = S \cdot {}^V_R Rot \cdot ({}^R P - {}^R P_0) + {}^V P_0 \quad (1)$$

where  $P$  is a point of interest;  ${}^V_R Rot$  is the rotation matrix from the robot to the video coordinate frame; and  $S$  is the scaling matrix. These were defined as:

$${}^V_R Rot = \begin{bmatrix} \cos \theta & -\sin \theta \\ \sin \theta & \cos \theta \end{bmatrix} \quad (2)$$

$$S = \begin{bmatrix} S_X & 0 \\ 0 & S_Y \end{bmatrix} \quad (3)$$

The scaling factors  $S_X$  and  $S_Y$  were measured in pixels/micrometers. They were computed using Eq. 1 and the acquired points  $P_0$  and  $P_1$ .

After this initial mapping estimation, the entire set of reference points was used to improve the mapping parameters. This was achieved by minimization of the error function defined by (4), which represents the RMS error between the real and the computed tool positions in robot coordinates.

$$\epsilon = \sqrt{\frac{\sum_{i=0}^n \left\{ \left( {}^R \hat{X}_i - {}^R X_i \right)^2 + \left( {}^R \hat{Y}_i - {}^R Y_i \right)^2 \right\}}{n}} \quad (4)$$

In (4),  $({}^R X_i, {}^R Y_i)$  represents the  $i^{th}$  actual x-y robot position,  $({}^R \hat{X}_i, {}^R \hat{Y}_i)$  represents the  $i^{th}$  computed x-y robot position, and  $n$  is the number of calibration points used for the computations.

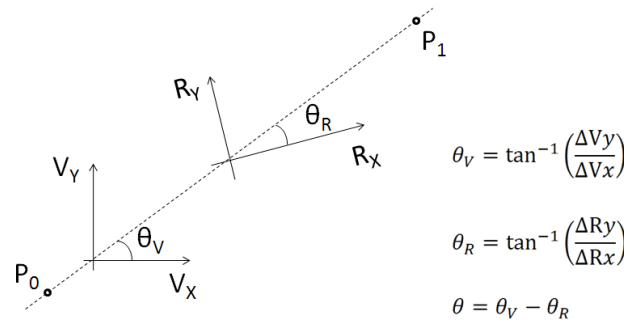


Fig. 6: Method used to compute the rotation between the robot and the video coordinate frames.  $P_0$  and  $P_1$  were points with known coordinates on both frames.

## V. TRAINING SCENARIOS

The main goal of the developed training scenarios was familiarize new users with the teleoperated system environment, introducing them to the system control and joystick functions. Training using mixed-reality is a safe, fast and inexpensive way of developing the necessary control skills with new operators. Therefore, two tasks were developed to provide the basic training that could guarantee high levels of performance and safe operations even on the very first real biomanipulations.

For evaluation purposes, both tasks always start at the same point, i.e., with the pipette tip inside a fixed virtual home region (see Fig. 5). In addition, the last task of a training session has the exact same configuration (in terms of target locations or trajectory to be followed) as the first test attempted, enabling a fair comparison between initial and final operator performances.

#### A. Move-and-inject scenario

This task was created to focus operator training on precise teleoperated positioning of the pipette tip. In this case, several virtual targets are randomly overlaid on the live video captured from the microscope's field of view, as shown in Fig. 5. The task of the operator is to move the pipette's tip to each of these targets. When the pipette is over a target, the operator should "inject" it by pressing the joystick's trigger button. This action corresponds to an automatic injection motion when manipulating real cells, which is customizable in terms of distance, direction and speed, and is triggered by the same joystick button. When a target is successfully injected, it disappears from the screen. The operator's goal is to eliminate all targets displayed. Completion of this goal finalizes the task.

Different levels of difficulty can be set in this scenario by changing: 1) the number of targets; 2) the size of the targets; 3) the number of obstacles; 4) the size of the obstacles; and 5) the maximum time allowed to complete the task. Making the targets smaller increases task difficulty because it requires better precision in pipette positioning. The presence of obstacles also increases game difficulty because this means the user has to learn to control the pipette's trajectory, not simply go straight to the targets.

Experimental data collected during this task includes the pipette tip position in image coordinates, recorded at 25Hz; the number of collisions with virtual obstacles; and the total duration of the task, i.e., the amount of time spent to “inject” all targets. Saving the pipette tip positions enables offline analysis of the user’s skills and strategies. Here, these data were used to measure the total distance travelled by the pipette during the test, which was then normalized by the absolute minimum travel distance computed using a version of the travelling salesman algorithm. This normalized distance was used as a performance metric. In addition, the average pipette speed during the experiment was also computed and used as a performance metric.

**B. Trajectory following scenario**

The goal of this task was to train new users on the dynamic control of the micromanipulation pipette motions, focusing on speed and direction control skills. Here, a desired trajectory was randomly defined, but always started

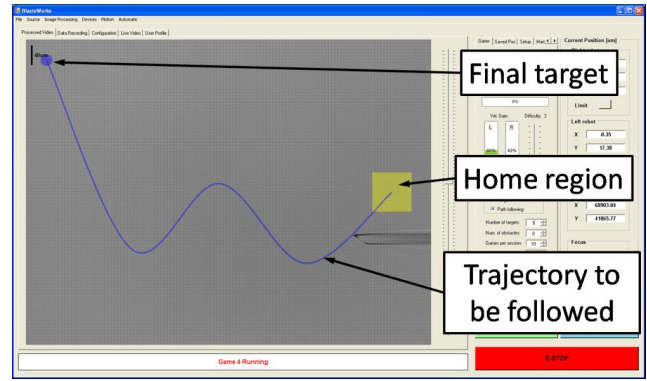


Fig. 7. The trajectory following game scenario.

in the centre of the home region and finished on a target located at the opposite side of the video panel. The operator’s task consisted of guiding the pipette tip from the

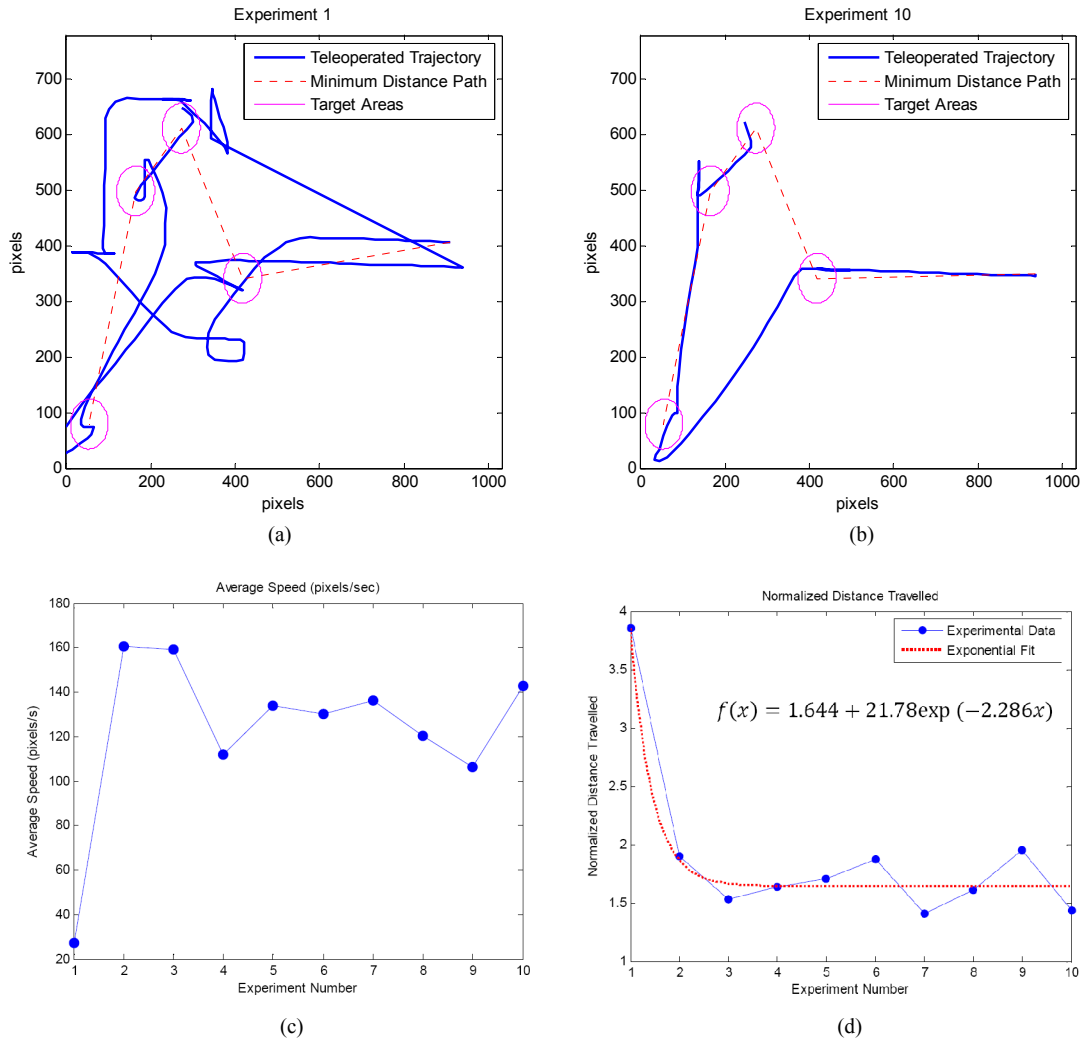


Fig. 8. Examples of game data and metrics collected for the move-and-shoot game played by a novice operator: (a) Data from the first training session game; (b) Data from the last training session game; (c) Average pipette speed on each game played; (d) Normalized distance travelled on each game played.

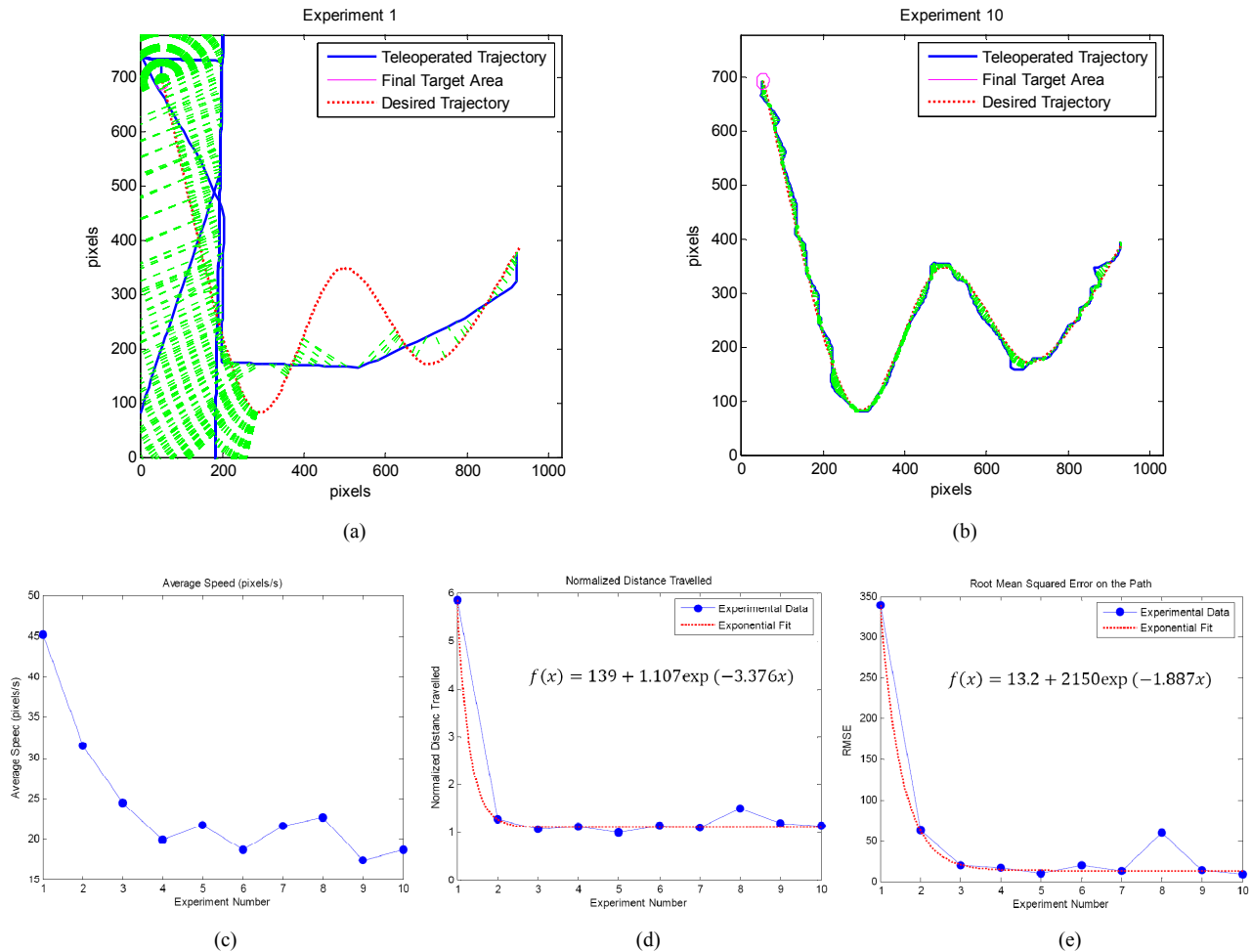


Fig. 9. Examples of task data and metrics collected for the trajectory following scenario played by a novice operator: (a) Data from the first training session, with green lines showing the smallest distance from a sampled pipette coordinate to the desired trajectory; (b) Data from the last training session; (c) Average pipette speed on each task played; (d) Normalized distance travelled; (e) RMSE of the trajectory following task.

home region to the final target following the given trajectory. A typical task is shown in Fig. 7.

As in the previous scenario, the difficulty level could also be adjusted. This was achieved by changing the number of waypoints selected for the trajectory definition. Increasing the number of waypoints creates more twists and turns on the desired trajectory, requiring better motion and speed control to achieve a good performance. The trajectory was defined using spline interpolation, i.e., as a smooth curve passing through all given waypoints. Randomness came from the fact that the y-coordinate of the waypoints were defined randomly (but not the x-coordinates – these were regularly spaced between the home region and the target).

Evaluation of the operator performance was based on the root-mean-squared-error (RMSE) between the trajectory followed and the desired trajectory. This error was computed offline, based on the recorded pipette tip coordinates. The error from a sampled pipette coordinate to the desired trajectory was assumed to be the smallest distance between

those two entities. This measure is represented by the green lines in Fig. 9, which displays experimental data from one of the novice operators.

Another two measures obtained from this task were the total distance travelled by the pipette and the amount of time required to complete the given task. These were used to generate two metrics: the average pipette speed; and the normalized distance travelled, which was computed using the length of the desired trajectory as the normalizing factor.

## VI. TRAINING EXPERIMENTS

The two mixed-reality training scenarios were used to train 20 totally novice operators on the control of the teleoperated biomanipulation system. All of these operators had no prior experience with biomanipulations or any other type of micromanipulation, and each of them went through only one training session in the teleoperated system. Here, a training session consisted of attempting only one of the scenarios 10 times. Therefore, the group of novice operators

was divided in two sets for the experiments: One half performed the move-and-shoot scenario and the other attempted the trajectory following scenario.

The difficulty level of the tasks was kept constant during the training sessions, and was the same for all users. For the move-and-shoot task, the number of targets selected was four; the diameter of the targets was set to 90 pixels; no obstacle was present; and there was no time limit to finish the task. For the trajectory following case, the desired path was defined from four random waypoints plus the fixed initial point at the centre of the home region. Once again there was no time limit to finish the task.

Examples of “move-and-inject” tests and of the data collected during a training session are shown in Fig. 8. Both the first and the last test completed by an operator are presented, from which a great performance improvement can be readily seen. The metrics obtained during this training session show an exponential learning curve, which was typical for operators that classified themselves as non video game players. On average, operators reached a performance level within 10% of their final performance by the third test. An interesting observation was the good performance of operators that classified themselves as gamers. In these cases, little improvement was noticed during the training sessions because these operators performed well from their very first trial.

An example of a trajectory following training session is presented in Fig. 9. In this case a great performance improvement is also clearly seen when comparing data from the first and last games played by the operator. Additionally, the experimental metrics show, once again, an exponential learning curve, which was typical for the non-gamer operators. This learning trend allows us to conclude that the teleoperated biomanipulation system is user-friendly and easy to operate.

The overall average of the trajectory following RMSE computed for all operators decreased from an initial 66.9 pixels to a final 20.3 pixels, demonstrating an error reduction of almost 70% after only one training session. In addition, the overall change in normalized distance travelled between the first and the last scenario of the training sessions was -25.2% for the move-and-inject task, and -21.5% for the trajectory following task, indicating good improvements in pipette motion control for both groups of operators. Another interesting observation from overall average data was the speedup measured for the move-and-inject scenario. On average, the operators are 66.3% faster in precise pipette positioning after undergoing the move-and-inject training session. A much smaller speedup was found for the trajectory following scenario, only 5.5%, which can be explained by the fact that operators learned to keep the speed low to better control the pipette trajectory. These data are summarized in Table I.

## VII. CONCLUSION AND FUTURE WORK

A mixed-reality training system for teleoperated biomanipulations has been developed and tested during this research. The training platform consisted of a previously

TABLE I. OVERALL AVERAGE OF GAME METRIC CHANGES<sup>A</sup>

Metric	Percentage Change	
	<i>Move-and-shoot game</i>	<i>Trajectory following game</i>
Average Speed	+66.3%	+5.5%
Normalized Distance Travelled	-25.2%	-21.5%
Trajectory Following RMSE	—	-48.9%

a. computed from data from the first and last games played by each operator.

developed fully teleoperated biomanipulation system, which was augmented by a new mixed-reality interface developed for operator training. Here, the biomanipulation system provided the real setting for training, while virtual targets and virtual obstacles replaced the real cells to be manipulated. Setup time for training in this system was short, only 3 to 5 minutes, and the pipette was practically impossible to break because it was positioned far away from any physical obstacle.

Two mixed-reality training scenes were designed, implemented and tested during this research: One focused on precise positioning training using a “move-and-inject” task; and the other aimed to develop precise motion control skills in new operators, based on trajectory following tasks. Results from preliminary experiments with 20 totally novice operators demonstrated that this training system was effective in terms of initial development of the necessary control skills for real teleoperated biomanipulations. Training here was shown to be fast, safe, and inexpensive since no real cells, biochemical products, or pipettes were needed for this initial phase.

The experiments demonstrated that learning on this new system was exponential, enabling operators to reach, on average, a performance level within 10% of their final performance by the third training run. In addition, all operators were able to achieve precise positioning at an average rate greater than 8.18 targets/min, and trajectory following with RMSE less than 27.9 pixels after only 10 practice runs. Furthermore, operators that classified themselves as gamers demonstrated this level of performance from their very first trial. These observations not only reiterated that training on the developed mixed-reality system is fast, but also tells us that, as younger generations become more familiar with games, virtual realities, and the use of technologies, the value of a teleoperated system that feels like a computer game tends to increase.

Future training sessions will evaluate the impact of progressively increasing the level of difficulty of the developed scenarios. The goal will be to maintain the operator’s initial learning rate for a longer period of time, hopefully taking their final control skills to a more advanced level without increasing the number of practice sessions. In addition, a group of operators will be trained on a mix of both scenarios, and later will be asked to perform real cell

microinjections. This will be the final training system test, which will evaluate the hypothesis that teleoperated skills acquired in the mixed-reality trainer do transfer to real biomanipulations.

## REFERENCES

- [1] L. S. Mattos and D. G. Caldwell, "A Mixed Reality Training System for Teleoperated Biomanipulations," *Proceedings of International Conferences on Advances in Computer-Human Interactions*, ACHI 2010, February 2010.
- [2] D. Kim, S. Yun, B. Kim, "Mechanical force response of single living cells using a microrobotic system," *2004 IEEE International Conference on Robotics and Automation*, New Orleans, USA, April 2004.
- [3] A. Kapoor, R. Kumar, R. H. Taylor, "Simple biomanipulation tasks with Steady Hand cooperative manipulator," *Medical Image Computing and Computer-Assisted Intervention - MICCAI 2003*, Lecture Notes in Computer Science, vol. 2878, pp. 141-148, ISBN: 3-540-20462-8, 2003.
- [4] N. Stylopoulos and D. Rattner, "Robotics and ergonomics," *Surgical Clinics of North America*, vol. 83(6), pp. 1321-1337, 2003.
- [5] S. Ogawa, H. Takahashi, J. Mizuno, N. Kashiwazaki, M. Yamane, E. Narishige, "Personal computer-controlled microsurgery of fertilized eggs and early embryos," *Theriogenology*, vol. 25(2), 1986.
- [6] L. Mattos and D.G. Caldwell, "Interface design for microbiomanipulation and teleoperation," *Second International Conference on Advances in Computer-Human Interactions*, ACHI 2009, Mexico, February 2009.
- [7] D. Kim, B. Kim, S. Yun, and S. Kwon, "Cellular force measurement for force reflected biomanipulation," *2004 IEEE International Conference on Robotics and Automation*, New Orleans, USA, April 2004.
- [8] A. Pillarisetti, M. Pekarev, A. D. Brooks, J. P. Desai, "Evaluating the effect of force feedback in cell injection," *IEEE Transactions on Automation Science and Engineering*, Vol. 4, No. 3, July 2007.
- [9] G. H. Ballantyne and F. Moll, "The da Vinci telerobotic surgical system: the virtual operative field and telepresence surgery," *Surgical Clinics of North America*, vol. 83(6), pp. 1293-1304, 2003.
- [10] L. B. Rosenberg, "Virtual fixtures: Perceptual tools for telerobotic manipulation," *IEEE Virtual Reality Annual International Symposium*, pp. 76-82, 1993.
- [11] O. Tonet, M. Marinelli, G. Megali, A. Sieber, P. Valdastrì, A. Menciassi, P. Dario, "Control of a teleoperated nanomanipulator with time delay under direct vision feedback," *2007 IEEE International Conference on Robotics and Automation*, pp. 3514-3519, Rome, Italy, 2007.
- [12] X.Y. Liu, K.Y. Kim, Y. Zhang, and Y. Sun, "NanoNewton force sensing and control in microrobotic cell manipulation," *International Journal of Robotics Research*, vol. 28(8), pp. 1065-1076, 2009.
- [13] N. Turro, O. Khatib, E. Coste-Maniere, "Haptically Augmented Teleoperation," *2001 IEEE International Conference on Robotics and Automation*, pp. 386- 392, 2001.
- [14] N. Garcia-Hernandez and V. Parra-Vega, "Haptic Teleoperated Robotic System for an Effective Obstacle Avoidance," *Second International Conference on Advances in Computer-Human Interactions*, ACHI 2009, Mexico, February 2009.
- [15] B.L. Davies, S. Harris, M. Jakopec, J. Cobb, "A novel hands-on robot for knee replacement surgery," *Computer Assisted Orthopaedic Surgery USA* (CAOS USA), A. DiGioia and B. Jaramaz, Eds. Pittsburgh: UPMC Medical Center, pp. 70-74, 1999.
- [16] A.K. Bejczy, W.S. Kim, S. Venema, "The phantom robot: predictive displays for teleoperation with time delay," *1990 International Conference on Robotics and Automation*, 1990.
- [17] M. Ammi, A. Ferreira, J-G. Fontaine, "Virtualized reality interfaces for telemicromanipulation," *2004 IEEE International Conference on Robotics and Automation*, New Orleans, USA, April 2004.
- [18] Finnair Flight Training Center, [www.finnairflighttraining.com](http://www.finnairflighttraining.com)
- [19] G. Lacey, D. Ryan, D. Cassidy, D. Young, "Mixed-reality simulation of minimally invasive surgeries," *IEEE MultiMedia*, vol.14(4), p.76-87, October 2007.
- [20] K. Jayapal, K. Wlaschin, M. Yap, W-S Hu, "Recombinant protein therapeutics from CHO cells - 20 years and counting," *Chemical Engineering Progress*, vol. 103(7), October, 2007.
- [21] L. Mattos and D. G. Caldwell, "A fast and precise micropipette positioning system based on continuous camera-robot recalibration and visual servoing," *IEEE Conference on Automation Science and Engineering*, CASE 2009, August 2009.